Active and Selective Bifunctional Catalyst for Gasoline Production through a Slurry-Phase Fischer–Tropsch Synthesis

ARTICLE *in* INDUSTRIAL & ENGINEERING CHEMISTRY RESEARCH · SEPTEMBER 2007

Impact Factor: 2.59 · DOI: 10.1021/ie070099j

4 AUTHORS, INCLUDING:

Chawalit Ngamcharussrivichai
Chulalongkorn University
35 PUBLICATIONS **701** CITATIONS
SEE PROFILE

Apichat Imyim
Chulalongkorn University
27 PUBLICATIONS **452** CITATIONS
SEE PROFILE

Kaoru Fujimoto
Kitakyushu University
366 PUBLICATIONS **7,001** CITATIONS
SEE PROFILE

Active and Selective Bifunctional Catalyst for Gasoline Production through a Slurry-Phase Fischer−Tropsch Synthesis

Chawalit Ngamcharussrivichai,[†] Apichat Imyim,[‡] Xiaohong Li,[§] and Kaoru Fujimoto*[,§]

Fuels Research Center, Department of Chemical Technology, Faculty of Science and Department of Chemistry, Faculty of Science, Chulalongkorn University, Bangkok 10330, Thailand, and Department of Chemical Processes and Environments, Faculty of Environmental Engineering, The University of Kitakyushu, Kitakyushu, Fukuoka 808-0135, Japan

Catalytic performance of various bifunctional Co-based catalysts has been investigated in a slurry-phase Fischer−Tropsch synthesis at 1 MPa and 230 °C. The catalysts were prepared according to the conventional impregnation method using SiO_2, Al_2O_3, montmorillonite (K10), and various zeolites (USY, ZSM-5, and MCM-22) as supports. Characterizations by XRD, N_2 adsorption−desorption, H_2-TPR, SEM, and TEM suggested the presence of at least two locally different Co species in the zeolite-supported catalysts: one with large particle sizes located on the external surface of the supports and the other one with small crystallites fixed inside the micropores. Co/MCM-22 catalysts exhibited high reducibility due to the small particle size of MCM-22 support that can accommodate more reducible active Co oxides with large crystal sizes on its external surface. It was found that the selectivity to long-chain hydrocarbon products was retarded obviously, and the carbon number distribution was shifted to gasoline range (C_4−C_{12}) when an acidic support was applied. The bifunctional catalysts also enhanced the selectivity to isoparaffins. Co/MCM-22 showed a superior CO conversion and selectivity to gasoline-range products and isoparaffins to other zeolite-supported Co catalysts. Its hydrogenation activity and hydrocarbons selectivity depended on the SiO_2/Al_2O_3 ratio. Moreover, a mechanism of hydrocarbon formation over a zeolite-supported Co catalyst under the slurry-phase conditions was proposed.

Introduction

The Fischer−Tropsch (FT) synthesis is considered an effective process in producing a wide-range of liquid hydrocarbon fuels and high-value added chemicals from abundant resources, such as natural gas, coal, and biomass, via synthetic gas.[1] It has recently received more attention than ever, as a result of limited petroleum reservoirs and environmental constraints these days, since there is a significantly increasing interest in the production of ultraclean fuels for transportation, e.g., diesel and gasoline.[2−4] However, the FT products are controlled by the Anderson-Schulz-Flory (ASF) polymerization kinetics, resulting in a nonselective formation of any hydrocarbons.

Various combinations of active FT metals, i.e., Fe, Co, and Ru, and acidic function containing materials have been extensively investigated in order to circumvent the ASF distribution and to selectively produce high-octane gasoline-range hydrocarbons.[5−13] Due to their shape-selective properties and high acidity, zeolites, especially HZSM-5 with sinusoidal and straight 10-membered ring channels, have been often applied as a support for the FT catalysts. HZSM-5-supported Co catalysts show a good selectivity to aromatic and isoparaffin products, but the CO conversion is low.[12−14] This is attributed to low reducibility of the catalysts to the active form.[15] Even though many attempts have been made through various catalyst preparation and modification procedures, the resulting catalysts do not exhibit a remarkable improvement in activity.[8,9,12]

Reuel and Bartholomew revealed support effects on reducibility and metal dispersion of Co catalysts in the CO hydrogenation.[16] A strong interaction between Co and support with a high electron density surface lowered reducibility, retarding the FT reaction rates and enhancing the selectivity to methane. In contrast, Iglesia et al. showed that the activity in FT synthesis was proportional to the metal dispersion and almost independent of the support.[17,18] The C_{5+} selectivity increased with increasing the Co site density because of the diffusion-enhanced readsorption of primary α-olefin products. The size of support pores also critically altered the product selectivity via mass transfer restrictions of the syngas reactant.[19] The H_2/CO ratio could be increased within small pores, resulting in an increase in the formation of methane. It was also suggested that the small crystal zeolite support enhances the extent of secondary acid-catalyzed reactions.[14]

In the present study, we have investigated the performance of various acidic material-supported Co catalysts in a slurry-phase FT synthesis. MWW zeolites, so-called MCM-22 (Figure 1), with a very unique structure composed of two different pore channel systems, sinusoidal 10-membered ring channels and large supercages with a 10-membered ring pore entrance existing between sheet layers, have been applied as a support for the FT catalyst for the first time since it may be selective for gasoline synthesis in a similar manner to ZSM-5. Furthermore, its high external surface area derived from terminal 12-membered ring cuplike pores is expected to provide an alternative result. Interestingly, we found that MCM-22-supported Co catalysts with suitable physicochemical properties exhibited a superior performance to others, and the gasoline-range products can be actively and selectively produced under the slurry-phase conditions.

Experimental Section

Catalyst Preparation and Characterizations. Co catalyst (20 wt % Co) was prepared by the incipient wetness impregna-

* To whom correspondence should be addressed. E-mail: fujimoto@env.kitakyu-u.ac.jp.

[†] Department of Chemical Technology, Chulalongkorn University.

[‡] Department of Chemistry, Chulalongkorn University.

[§] The University of Kitakyushu.

10.1021/ie070099j CCC: $37.00
Published on Web 09/15/2007

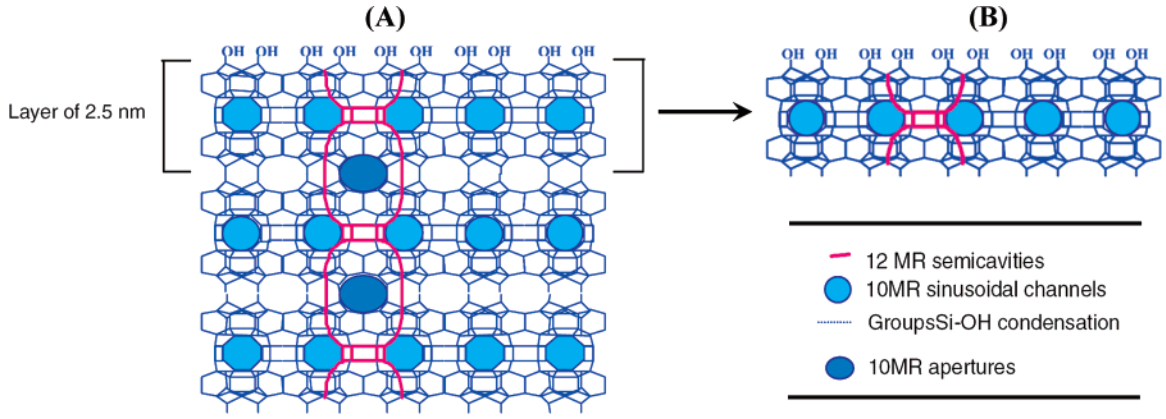

Figure 1. Schematic MWW-type structure of the MCM-22 zeolite; an array of sheet layers perpendicular to the *c*-axis to form the MWW structure (A) and a sheet layer with terminal 12-membered ring cuplike pores (B). (Adapted from ref 20.)

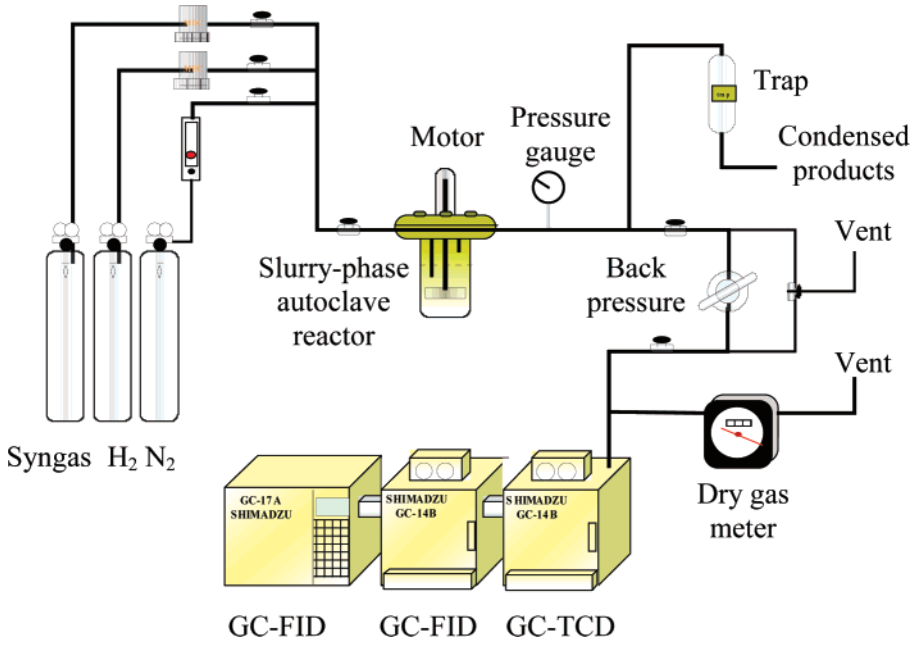

Figure 2. Schematic flow diagram of a slurry-phase FT synthesis apparatus.

tion of an aqueous solution of cobalt nitrate ($Co(NO_3)_2 \cdot 6H_2O$) on various supports. The supports used include silica gel (Fuji silycia), alumina (Sumitomo Chemical Co.), montmorillonite K10 (Aldrich), acid-form zeolites, i.e., USY and ZSM-5 with a SiO_2/Al_2O_3 ratio of 33 and 38, respectively (Tosoh), and our synthesized MCM-22 with a SiO_2/Al_2O_3 ratio of 30 and 50. After the support and the nitrate solution were well mixed, the sample was dried in a rotary evaporator for 30 min. It was then calcined in a muffle furnace at 400 °C for 2−5 h. Hereafter, the catalyst samples were designated as Co/*XXX* (*YY*), where *XXX* denotes the types of support and *YY* indicates the SiO_2/Al_2O_3 ratio.

MCM-22 zeolites with different SiO_2/Al_2O_3 ratios were hydrothermally synthesized according to the procedure reported by Corma et al.[21] Before being used as a support, the calcined MCM-22 was treated with a 1 M NH_4NO_3 solution 3 times at 80 °C for 3 h. A proton-form MCM-22 was attained by subsequent calcination at 500 °C for 5 h. DeMCM-22 with the SiO_2/Al_2O_3 ratio of 80 (DeMCM-22 (80)) was prepared by dealumination of MCM-22 (30) in an acidic solution. The typical procedure was dispersion of the parent MCM-22 into a 0.5 M HNO_3 solution with a solid-to-liquid ratio of 1:20 under vigorous stirring at 80 °C for 2 h. The procedure was repeated twice before the solution was dried at 120 °C overnight and calcined at 500 °C for 4 h in a muffle furnace.

The technique of powder X-ray diffraction (XRD) was applied to confirm the crystallinity of supported Co catalysts using a Rigaku DMAX 2200/Ultima+ diffractometer. Bulk elemental composition was determined by means of inductively coupled plasma (ICP). N_2 adsorption−desorption was measured on a Micromeritics ASAP 2020 surface area and porosity analyzer to characterize surface area, pore size, and pore volume. A JEOL JSM-5410 LV scanning electron microscope (SEM) was used for the investigation of catalyst morphologies. The crystallite size and structure of Co particles were analyzed with a JEM-100SX tuning electron microscope (TEM). The temperature programmed reduction (TPR) under flow of an H_2−Ar mixture was carried out in a Micromeritics ASAP 2029 chemisorb analyzer.

Reaction Apparatus and Procedure. The schematic diagram of the experimental apparatus used in the present study is shown in Figure 2. The FT synthesis was carried out in a 250-mL stainless steel autoclave. The mixture of H_2 and CO with a H_2/CO molar ratio of 2 (Sumitomo Chemical Co.) was used as a syngas reactant. For a typical procedure, 1 g of Co catalyst was activated ex situ at 400 °C for 10 h in H_2 gas with a flow rate

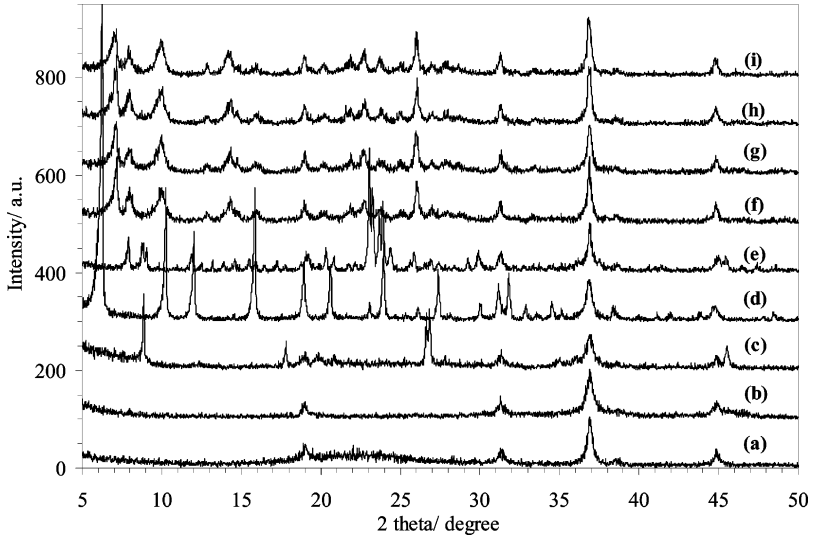

Figure 3. XRD patterns of our prepared Co catalysts: Co/SiO_2 (a), Co/Al_2O_3 (b), Co/MONT (c), Co/USY (d), Co/ZSM-5 (e), Co/MCM-22 (30) (f), Co/MCM-22 (50) (g), Co/DeMCM-22 (80) (h), and Co/NaMCM-22 (30) (i).

of 100 mL min^{-1}. The reduced catalyst was then transferred to the autoclave filled with 20 mL of n-hexadecane solvent. The flow rate of syngas was controlled and monitored using a Brooks 5850E mass flow controller. The operating conditions were $T = 230$ °C, $P = 1.0$ MPa, and $W/F = 5$ g_{cat} h mol^{-1}, and the stirring speed was maintained at 800 rpm. Effluent gas was passed through two consecutive traps to condense the remaining liquid products. The effluent gas flow rate was measured with a dry gas flow meter.

Products in the effluent gas were analyzed by three consecutive online gas chromatographs (GC). CO, CO_2, and CH_4 were analyzed with a GC equipped with a packed column and a thermal conductivity detector (TCD), while an amount of other gaseous hydrocarbon products was determined with two different GCs equipped with a packed column and a flame ionization detector (FID). After the course of reaction, the product distribution in liquid phase was analyzed with a FID GC equipped with a capillary column (DB-2881). The selectivity of hydrocarbons was calculated on the basis of the carbon number.

Results and Discussion

Characteristics of Bifunctional Catalysts. XRD patterns of various supported Co catalysts after the air calcination at 400 °C are shown in Figure 3. It can be seen that the structure and the crystallinity of montmorillonite and zeolite supports were retained after the impregnation of Co. The diffraction peaks which appeared at $2\theta = 19.0$, 31.3, 36.9, and 44.8° indicated clearly the presence of Co oxide with the form of Co_3O_4 in all the catalyst samples.[22] No peak related to the CoO phase ($2\theta = 42.5°$) was observed. Moreover, the shape and sharpness of the Co oxide peaks, especially at $2\theta = 36.9°$, suggested that the Co oxides formed on zeolite supports, except for USY, were more crystalline than those present on SiO_2, Al_2O_3, and montmorillonite. This result is consistent with the previous work reporting that the highly crystallized Co oxide particles were favored when using an oxide with a high electron density surface as the support.[23]

The textural properties of our supported Co catalysts are summarized in Table 1. SiO_2- and Al_2O_3-supported catalysts had a much larger pore size and pore volume than zeolite-supported catalysts, but the surface area of the former was lower. The USY-supported Co catalyst showed the highest surface area among the zeolite supports. This result was according to the fact that this zeolite has a more open structure and contains some mesoporosity. MCM-22 had a higher surface area than ZSM-5, although their channel structures and pore openings are similar: both have partly sinusoidal 10-membered ring channels. This result can be explained by a significant difference in the particle size of both zeolites as revealed by SEM images in Figure 4. It indicated that MCM-22 support with a thin platelike shape has a much smaller particle size (~0.4 μm) than ZSM-5 that has an average size particle of ~3.5 μm. This also suggested that MCM-22 zeolites have a higher external surface area. A larger surface area of support promotes well dispersion of active metal species loaded, which may affect the formation of light hydrocarbon products.[24] It was also suggested that the small crystal zeolite support enhances the extent of secondary acid-catalyzed reactions.[14]

Table 1. Textural Properties of Supported Co Catalysts Used in the Present Study

		textural properties			Co oxides size (nm)	
catalyst	SiO_2/Al_2O_3[a]	S_L[b] (m^2 g^{-1})	D_p[c] (nm)	V_p[d] (cm^3 g^{-1})	XRD	TEM
Co/SiO_2	−	108	42	1.10	29.1	16.7
Co/Al_2O_3	−	149	37	0.76	21.8	13.8
Co/MONT	nd[e]	282	0.70	0.23	25.0	15.9
Co/USY	33	696	0.76	0.35	26.9	15.0
Co/ZSM-5	38	330	0.51	0.16	29.6	13.9
Co/MCM-22 (30)	30	468	0.55	0.38	30.7	15.3
Co/MCM-22 (50)	51	461	0.54	0.37	31.3	16.8
Co/DeMCM-22 (80)	84	458	0.55	0.33	33.1	17.6
Co/NaMCM-22 (30)	30	471	0.55	0.40	30.7	14.8

[a] Determined by ICP. [b] Represents the Langmuir surface area. [c] Represents the average pore diameter. [d] Represents the average pore volume. [e] Means not detected.

Figure 5 illustrates high-angle XRD patterns of all supported Co catalysts. The diffraction peak at $2\theta = 65.3°$, corresponding to the (400) plane of Co_3O_4, was used for calculation of the Co oxide particle size according to Sherrer's equation.[25] As shown in Table 1, the calculated Co oxide size of Co/SiO_2 (29.1 nm) was higher than that of Co/Al_2O_3 (21.8 nm). This result is consistent with the report by Ernst et al., which revealed the dependence of the Co oxide crystal size on surface characteristics of support: the size of Co oxides decreases with increasing negative charge of the support surface through an interaction between the metal oxides and support surface.[26] Our

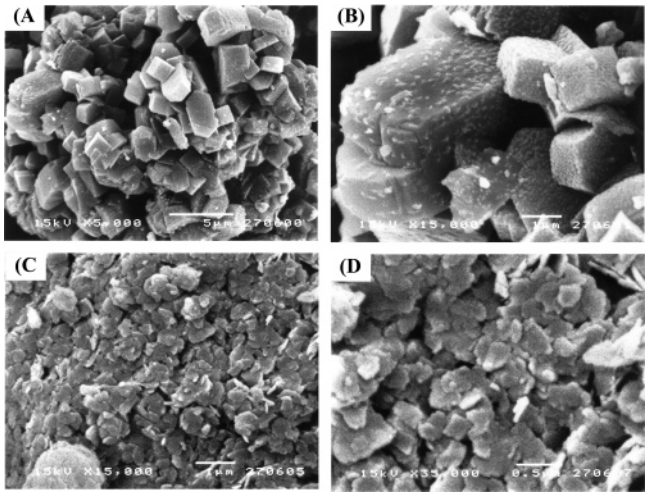

Figure 4. SEM images of Co/ZSM-5 (A and B) and Co/MCM-22 (30) (C and D).

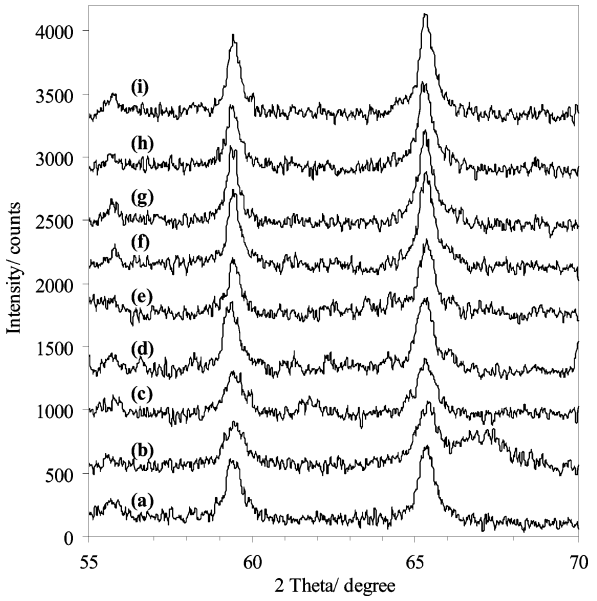

Figure 5. High-angle XRD patterns of Co catalysts: Co/SiO_2 (a), Co/Al_2O_3 (b), Co/MONT (c), Co/USY (d), Co/ZSM-5 (e), Co/MCM-22 (30) (f), Co/MCM-22 (50) (g), Co/DeMCM-22 (80) (h), and Co/NaMCM-22 (30) (i).

zeolite-supported Co catalysts possessed the average Co oxide sizes in the range of 25−33 nm. Among these, Co oxides in the Co/MCM-22 members exhibited slightly larger particle sizes. However, these observed Co oxides are much larger than the pore sizes of zeolitic supports themselves, suggesting that they must exist outside or on an external surface of the support particles. The study by means of the TEM technique indicated a wide range distribution of Co oxide particle sizes on the zeolite-supported catalysts with the average values between 13 and 18 nm (Figure 6 and Table 1), a half smaller than those calculated from the XRD patterns. These results implied the presence of at least two locally different Co oxides in the zeolite-supported catalysts. One with large particle sizes is located on the external surface of zeolitic supports. The other one with smaller sizes is formed from Co species diffusing into the zeolite channels and fixed inside the micropores. The latter Co oxides are difficult to be observed by TEM and may be X-ray invisible due to their very small crystallites.

Figure 7 shows H_2-TPR profiles of the supported Co catalysts after an in situ pretreatment at 400 °C. Theoretically, the reduction of Co_3O_4 to metallic Co should be a two-step process,

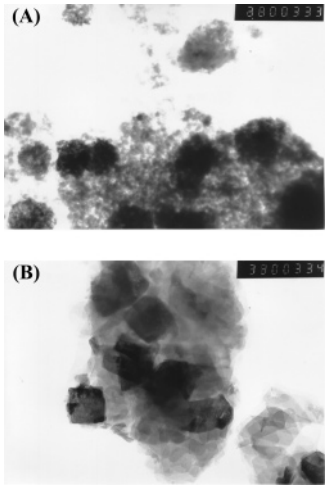

Figure 6. Comparison of TEM images of Co/SiO_2 (A) and Co/DeMCM-22 (80) (B) after air calcination at 400 °C (1 mm = 3 nm).

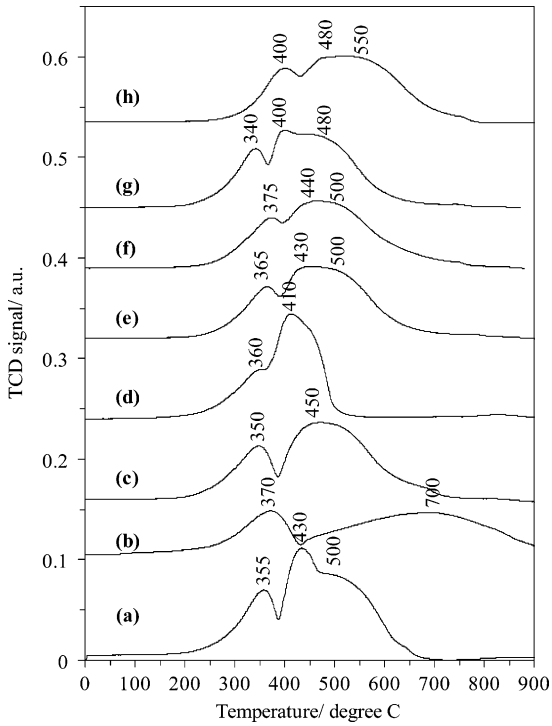

Figure 7. H_2-TPR profiles of various Co catalysts after air calcination at 400 °C: Co/SiO_2 (a), Co/Al_2O_3 (b), Co/USY (c), Co/ZSM-5 (d), Co/MCM-22 (30) (e), Co/MCM-22 (50) (f), Co/DeMCM-22 (80) (g), and Co/NaMCM-22 (30) (h).

giving two dominant peaks in a TPR profile. In practice, since the catalyst usually contains more than one single type of population of Co_3O_4 species, the two steps of reduction are superimposed, consequently appearing at different reduction temperatures. Except for the Co/Al_2O_3 catalyst, the Co catalysts exhibited mainly three peaks at around 350, 430, and 500 °C. The first peak is corresponding to the reduction of Co_3O_4 to CoO. The second peak can be assigned to the reduction of CoO to Co metal and further quantities of Co_3O_4 to CoO and, finally, the reduction of the remaining CoO to the Co metal.[27]

It can be seen that the TPR profile of Co/SiO_2 was similar to that of MCM-22-supported Co catalysts. However, the first and second peaks observed for Co/MCM-22 (30) and Co/MCM-22 (50) were significantly shifted to higher temperatures, indicating that the Co oxides present on zeolites were more difficult to be reduced to active Co species. With decreasing the aluminum

Table 2. Reducibility of the Cobalt Oxide Phase in Various Supported Co Catalysts Determined from the H_2-TPR Experiment

	reducibility of Co oxide phase (%)		
catalyst	T < 400 °C	T > 400 °C	total (rt−900 °C)
Co/SiO_2	36	62	98
Co/Al_2O_3	25	56	81
Co/USY	26	51	77
Co/ZSM-5	21	49	70
Co/MCM-22 (30)	30	56	86
Co/MCM-22 (50)	29	56	85
Co/DeMCM-22 (80)	40	51	91
Co/NaMCM-22 (30)	17	66	83

content of MCM-22 support (Co/DeMCM-22 (80)), all three peaks were shifted to lower temperatures, suggesting that Co oxides on DeMCM-22 (80) are easier to be converted to metallic Co than those on other MCM-22 members. It should be ascribed to the decrease in framework negative charge when the amount of aluminum decreased, weakening the interaction between Co oxides and the support surface.[16] Interestingly, the reduction peaks observed for Co/DeMCM-22 (80) appeared at even lower temperatures than those of Co/SiO_2, suggesting higher reducibility of the former. In contrast, the Na-form MCM-22-supported Co catalyst (Co/NaMCM-22 (30)) exhibited an increase in the reduction temperatures by 50 °C when compared with those of Co/SiO_2. This support, as a basic form zeolite, is supposed to possess the highest electron density framework. Hence, the reduction over Co/NaMCM-22 (30) may be the most difficult.

The Co/Al_2O_3 catalyst showed mainly two TPR peaks, while the second and third peaks for Co/USY and Co/ZSM-5 were overlapped. The first TPR peak for Co/USY and Co/ZSM-5 was located at similar temperatures to that for Co/SiO_2, whereas that for Co/Al_2O_3 was shifted to higher temperature (370 °C). A very broad peak with the center at 700 °C observed for Co/Al_2O_3 suggested a strong interaction of Co on Al_2O_3 as well as a formation of the cobalt-alumina phase, which is very difficult to reduce.[28] In the case of Co/ZSM-5, the first peak was very small, indicating a less amount of easily reduced Co oxides.

Table 2 summarizes the percentage of reducible Co oxides present in various supported Co catalysts. The data were calculated based on hydrogen consumption in the H_2-TPR experiment as early as described by Enache et al.[29] Reducibility of the Co oxide phase is defined as

$$\text{reducibility (\%)} = \frac{S_t}{S_{<T}} \times 100$$

where S_t is the theoretical reduction area. It is corresponding to the theoretical hydrogen consumption for a catalyst loaded with 20 wt % Co in the form of Co_3O_4. $S_{<T}$ is the experimental reduction area. It is estimated from the real hydrogen consumption obtained at temperatures below T. In this case, T is designated as the reduction temperature of Co catalysts in the reaction experiment (T = 400 °C).

From Table 2, it can be seen that, within the reduction temperature of 400 °C (T < 400 °C), Co/DeMCM-22 (80) possessed the most reducible active Co phase, slightly higher than Co/SiO_2. Moreover, the Co/MCM-22 members, except for Co/NaMCM-22 (30), exhibited higher reducibility than Co/Al_2O_3 and other zeolite-supported Co catalysts. The high reducibility of MCM-22-supported Co catalysts should be derived from the smaller particles and high surface area of the MCM-22 zeolite which can accommodate more large Co oxide particles on the external surface since these Co oxide species

Table 3. CO Conversion and Product Selectivity in Slurry-Phase Fischer−Tropsch Synthesis[a] over Various Supported Co Catalysts

			selectivity (%)		
catalyst	max. CO conversion (%)	CO conversion at 5 h (%)	C_1-C_3	C_4-C_{12}	C_{12+}
Co/SiO_2	66.2	54.2	15.9	36.6	47.5
Co/Al_2O_3	54.6	52.1	14.4	36.1	49.5
Co/MONT	57.9	57.8	21.9	43.3	34.8
Co/USY	49.2	37.0	31.1	49.7	19.2
Co/ZSM-5	21.1	18.2	29.2	48.1	22.7
Co/MCM-22 (30)	66.4	48.3	22.8	60.7	16.5
Co/MCM-22 (50)	67.6	58.2	22.4	53.8	23.8
Co/DeMCM-22 (80)	73.5	59.8	23.6	52.1	24.3
Co/NaMCM-22	60.6	42.1	26.9	53.4	19.7

[a] Reaction conditions: temperature, 230 °C; pressure, 1.0 MPa; W/F, 5.0 g h mol^{-1}; catalyst amount, 1.0 g; time, 5 h.

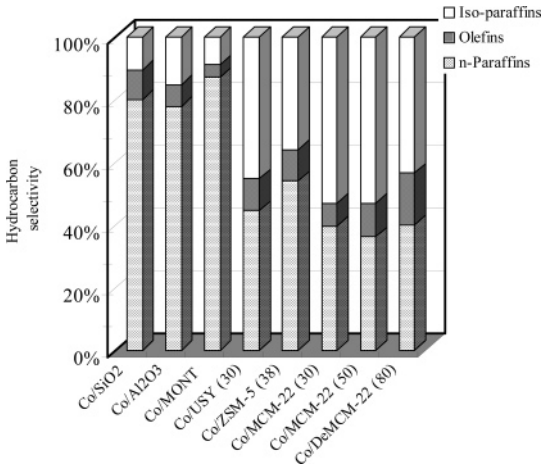

Figure 8. Distribution of hydrocarbon species in the FT synthesis over various Co catalysts.

are more easily reduced than those present as small crystallites inside the zeolitic micropores.[30]

It was also found that the reducibility for the entire reduction temperature range (up to 900 °C) observed for Co/USY and Co/ZSM-5 (70−77%) was lower than that for the Co/MCM-22 members (85−91%). This result indicated a higher amount of unreducible Co species in the USY- and ZSM-5-supported catalysts. Huang and Anderson reported that the introduced metal ions interact strongly with cation exchanged sites of ZSM-5 and cannot be reduced to metallic form.[31] Therefore, the relatively small amount of reducible active phase in Co/USY and Co/ZSM-5 should be ascribed to a high degree of ion exchange during the Co impregnation.

Loss of reducible Co species by the ion exchange should not only decrease the CO hydrogenation activity of the resulting catalyst but also decrease the support acidity. By carrying out additional temperature-programmed desorption of NH_3 (NH_3-TPD), the observed acid amounts of Co/USY and Co/ZSM-5 were 0.54 and 0.48 mmol NH_3 g^{-1}, respectively, whereas that of Co/MCM-22 (30) was 0.71 mmol NH_3 g^{-1}. Moreover, the strong interaction between the Co species and the zeolitic surface of USY and ZSM-5 was partially evident from the color of the Co impregnated zeolites after the final air calcination at 400 °C for 2 h. The pink color of Co^{2+} remained in the calcined Co/USY and Co/ZSM-5, whereas the calcined Co/MCM-22 members exhibited only a dark brown or a black color of Co oxides.

Co/NaMCM-22 (30) had the lowest reducible active Co phase at 400 °C (17%). This result should be attributed to a strong interaction between the Co species and the NaMCM-22

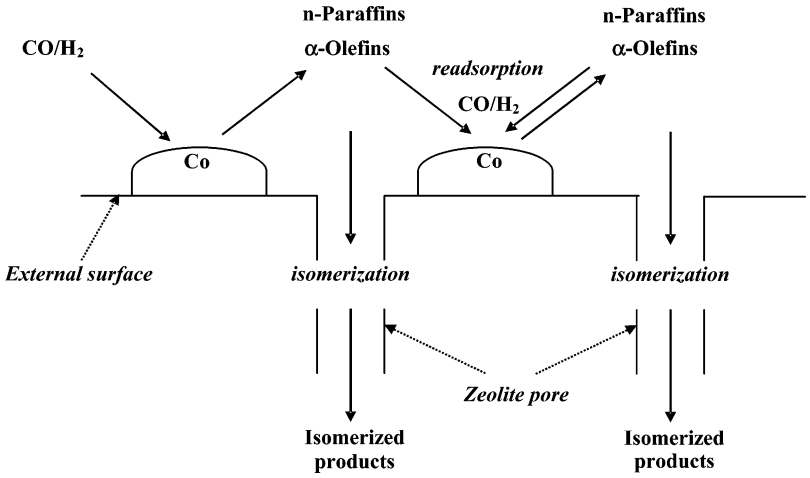

Figure 9. Schematic representation of proposed hydrocarbon formation mechanism under our study conditions.

framework as mentioned above. However, its reducibility from room temperature to 900 °C was comparable to other Co/MCM-22 catalysts. It implied that the ion exchange in NaMCM-22 occurred at a relatively small extent when compared with the case of Co/USY and Co/ZSM-5. It is worth noting that Co/NaMCM-22 possessed some acidity as determined by NH_3-TPD (0.62 mmol NH_3 g^{-1}), while NaMCM-22 itself did not chemically adsorb ammonia. This result suggested that the Na-form MCM-22 support is partly converted to the proton form during the impregnation. The presence of both H^+ and Na^+ may compete with Co^{2+} for ion exchanged sites, decreasing the amount of unreducible Co species.

Performance of Bifunctional Catalysts in the Fischer−Tropsch Synthesis. The CO conversion and product selectivity in the slurry-phase FT synthesis over various supported Co catalysts are summarized in Table 3. Co/SiO_2 showed the maximum CO conversion at 66.2% with a decline in the activity at a prolonged reaction time. After 5 h, the conversion became stable at 54.2%. Other catalysts also exhibited a similar change of the conversion with time. Therefore, the data up to 5 h were reported here. The main products over Co/SiO_2 were C_{12+} normal paraffins (see also Figure 8) with the selectivity of 47.5%, and the C_1-C_3 selectivity was 15.9%. Co/Al_2O_3 exhibited a similar product distribution to Co/SiO_2, but the CO conversion was lower. This result should be attributed to the lower reducibility of Co oxides on Al_2O_3 support (Figure 7 and Table 2).

In all cases, using the acidic supports resulted in an increase in the C_1-C_3 selectivity, predominantly over Co/USY and Co/ZSM-5 catalysts. This result should be mainly ascribed to the support acidity that can promote cracking of hydrocarbons once formed, resulting in an enhanced formation of the C_1-C_3 species. Among the zeolite-supported catalysts, the Co/MCM-22 members exhibited the lowest C_1-C_3 selectivity. The mass transfer gradient of syngas reactant within microporous channels[19] cannot account for these results since both ZSM-5 and MCM-22 have a similar channel structure and USY even possesses larger pore sizes (Table 1). It is likely to be due to the reducibility of Co oxides in catalysts. As shown in Table 2, Co/USY and Co/ZSM-5 have a lower reducibility than Co/MCM-22 catalysts. Reuel and Bartholomew reported that the formation of methane is enhanced over the catalyst with low reducibility.[16]

Co/MONT, Co/USY, and Co/ZSM-5 rendered the selectivity to gasoline-range hydrocarbons (C_4-C_{12}) increased concomitantly with a remarkable decrease in the C_{12+} selectivity. Their CO conversions were very low when compared to that of the Co/SiO_2 catalyst. The low conversions for these catalysts should be ascribed to the low reducibility as discussed in Figure 7 and Table 2. On the other hand, the shift of hydrocarbon selectivity to the C_4-C_{12} range should be due to microporous confinement and acidic properties of the zeolitic supports that limit the chain length of hydrocarbon products and catalyze cracking and isomerization reactions, respectively. It should be noted that, after we investigated the cracking performance of the zeolites under our studied conditions in the absence of syngas, it was found that a small amount of cracked products, mainly C_4-C_{12} hydrocarbons, derived from the n-hexadecane solvent was detected, corresponding to only 5−10% product yields. These results ensured that, under the slurry-phase synthesis conditions, the solvent cracked products have a minor contribution to the carbon number distribution.

MCM-22-supported Co catalysts exhibited a superior performance to other catalysts supported by zeolites. Due to the high reducibility, their maximum CO conversions were high, 60−73%. The conversion was dependent on the SiO_2/Al_2O_3 ratio of MCM-22 support. With decreasing the aluminum content (or increasing the SiO_2/Al_2O_3 ratio), the CO conversion over Co/MCM-22 catalysts increased. Interestingly, Co/DeMCM-22 (80) gave an even higher conversion than Co/SiO_2 at steady-state conditions (after 5 h). It should be accounted for with the increase in the extent of reducibility with decreasing the aluminum content (Table 2). On the other hand, Co/NaMCM-22 (30) with relatively high reduction temperatures required showed the lowest CO conversion. The results of the TPR experiment (Figure 7 and Table 2) discussed above correlated well with the catalytic activity results attained here.

The selectivity to C_4-C_{12} hydrocarbons obtained from Co/MCM-22 members increased to 50−60%, higher than other zeolite-supported Co catalysts. However, it was found that there is no significant difference in the C_{12+} selectivity regardless of the type of zeolitic supports. It is likely that the improvement of gasoline-range product selectivity over Co/MCM-22 catalysts is derived from the decrease in the selectivity to C_1-C_3 hydrocarbons. This observation suggested that the acidity of catalysts may not play the major role in control of the carbon chain length of the products since the amount of acid sites in Co/MCM-22 (30) (0.71 mmol NH_3 g^{-1}) was higher than that of Co/ZSM-5 (0.48 mmol NH_3 g^{-1}). Possibly, the product-size selectivity is particularly related to the reducibility and the zeolitic micropore confinement of catalysts.

The hydrocarbon species distribution in Figure 8 indicated n-paraffins as the major products obtained over low acidic Co/

SiO_2, Co/Al_2O_3, and Co/MONT catalysts. As a result of the support acidity, the selectivity to isoparaffins, high octane number species, was enhanced over the zeolite-supported Co catalysts. Moreover, over these bifunctional catalysts, the selectivity to olefins slightly increased. It was reported that 1-olefins are the dominant product from hydrocarbon formation within the zeolite pores where small metal clusters with low hydrogenation ability are present.[32] The maximum isoparaffin selectivity was achieved over Co/MCM-22 (30) (53%), while Co/ZSM-5 showed the lowest selectivity to isoparaffins (36%). Since the isomerization reaction is catalyzed over acid sites, this result should be attributed to the catalyst acidity.[33] The NH_3-TPD results confirmed the highest acidity of Co/MCM-22 (30) (0.71 mmol NH_3 g^{-1}). The effect of the number of acid sites in the catalysts on the extent of isomerization was also revealed over Co/MCM-22 catalysts with different SiO_2/Al_2O_3 ratios. With decreasing the amount of acid sites or increasing the SiO_2/Al_2O_3 ratio, the selectivity to isoparaffins was decreased. From the present study, Co/MCM-22 (30) is the most suitable catalyst for the active and selective production of gasoline-range hydrocarbons.

According to the FT synthesis under the present conditions, a schematic representation of hydrocarbon formation is proposed in Figure 9. The chain-growth mechanism for the formation inside zeolite pores was postulated elsewhere.[9] In such a case, the amount of hydrocarbons produced is very small due to the small Co clusters in the microporous channels and low reducibility of the catalyst prepared. On the other hand, in our case, the large Co metal particles on the external surface should promote the hydrogenation of CO more actively to olefins and paraffins. Readsorption of the olefins on the metallic Co causes carbon insertion and/or hydrogenation of the olefins to longer chain hydrocarbons and n-paraffins, respectively. The acid sites in the vicinity of Co particles can catalyze isomerization of the products formed through the diffusion into zeolitic micropores or near pore mouths.[14] MCM-22 with a small particle size should accommodate more of the large Co particles on an external surface area concomitantly while maintaining the acid sites within its microporous channels for isomerization. These large Co particles are more reducible and essential for the formation of C_{5+} hydrocarbons.[30] However, very long-chain hydrocarbons formed outside have a slow diffusion in the liquid medium and may not be structurally modified by the internal acid sites. This is reflected by the presence of a small amount of hydrocarbons with a chain length of more than 30 carbon atoms.

Conclusions

The physicochemical properties and performance of Co-based catalysts prepared by using various aluminosilicate materials as the supports in the slurry-phase FT synthesis at 1.0 MPa and 230 °C have been investigated. From the catalyst characterizations, compared to the case of the Co/SiO_2 catalyst, the impregnation of Co on zeolite supports resulted in the formation of relatively high crystalline Co oxides. A part of these oxides is in the form of cubic CoO as evidenced by TEM. The observed particle sizes of Co oxides suggested the presence of at least two locally different Co species in the zeolite-supported catalysts: one with large particle sizes located on the external surface of the supports and the other one with small crystallites fixed inside the micropores. The Co/MCM-22 members, except for Co/NaMCM-22 (30), showed higher reducibility at 400 °C than Co/USY and Co/ZSM-5 catalysts. The high reducibility should be derived from the small particle size of MCM-22 that can accommodate more reducible active Co oxides with large crystal sizes on its external surface.

Due to micropore confinement and acidity of the supports, the C_{12+} selectivity was remarkably decreased when the zeolite-supported Co catalysts were used. It is likely that the reducibility and zeolitic channel structure control the product selectivity to the C_4-C_{12} range. As a result of high reducibility, Co/MCM-22 catalysts are active for the conversion of CO. The conversion depends strongly on the SiO_2/Al_2O_3 ratio of MCM-22 support. The isoparaffin products are selectively produced over the Co/MCM-22 members with relatively high acidity. From the present study, the most suitable catalyst is Co/MCM-22 (30) that gave the gasoline-range hydrocarbon selectivity of 60% and the selectivity to isoparaffins of 53%. The small size MCM-22 support should promote the formation of long-chain hydrocarbons via hydrogenation and readsorption of primary olefin products over large Co particles on its external surface and encourage the secondary acid-catalyzed isomerization on the internal acid sites via diffusion into its microporous channels or near pore mouths.

Acknowledgment

The authors are grateful for the financial support from OECF-JBIC under the Thailand−Japan Technology Transfer Project (TJTTP) and Grants for Development of New Faculty Staff, Chulalongkorn University.

Literature Cited

(1) Vannice, M. A. The catalytic synthesis of hydrocarbons from carbon monoxide and hydrogen. *Cat. Rev.−Sci. Eng.* **1976**, *14*, 153.

(2) Weyda, H.; Kohler, E. Modern refining concepts—an update on naphtha- isomerization to modern gasoline manufacture. *Catal. Today* **2003**, *81*, 51.

(3) Tsubaki, N.; Yoneyama, Y.; Michiki, K.; Fujimoto, K. Three-component hybrid catalyst for direct synthesis of isoparaffin via modified Fischer-Tropsch synthesis. *Catal. Commun.* **2003**, *4*, 108.

(4) Matsuda, T.; Sakagami, H.; Takahashi, N. H_2-reduced Pt/MoO_3 as a selective catalyst for heptane isomerization. *Catal. Today* **2003**, *81*, 31.

(5) Bi, Y.; Dalai, A. K. Selective production of C4 hydrocarbons from syngas using $Fe\text{-}Co/ZrO_2$ and SO_4^{2-}/ZrO_2 catalysts. *Can. J. Chem. Eng.* **2003**, *81*, 230.

(6) Fraenkel, D.; Gates, B. C. Shape-selective Fischer-Tropsch synthesis catalyzed by zeolite-entrapped cobalt clusters. *J. Am. Chem. Soc.* **1980**, *102*, 2478.

(7) Botes, F. G.; Böhringer, W. The addition of HZSM-5 to the Fischer-Tropsch process for improved gasoline production. *Appl. Catal., A* **2004**, *267*, 217.

(8) Zhang, Z.; Yin, Y. G.; Sachtler, W. M. H. A novel preparation method for zeolite encaged Co clusters. *Catal. Lett.* **1993**, *18*, 73.

(9) Koh, D. J.; Chung, J. S.; Kim, Y. G. Selective synthesis and chain growth of linear hydrocarbons in the Fischer-Tropsch synthesis over zeolite-entrapped cobalt catalysts. *Ind. Eng. Chem. Res.* **1995**, *34*, 1969.

(10) Li, X.; Luo, M.; Asami, K. Direct synthesis of middle iso-paraffins from synthesis gas on hybrid catalysts. *Catal. Today* **2004**, *89*, 439.

(11) Li, X.; Asami, K.; Luo, M.; Michiki, K.; Tsubaki, N.; Fujimoto, K. Direct synthesis of middle iso-paraffins from synthesis gas. *Catal. Today* **2003**, *84*, 59.

(12) Jothimurugesan, K.; Gangwal, S. K. Titanium-supported bimetallic catalysts combined with HZSM-5 for Fischer-Tropsch synthesis. *Ind. Eng. Chem. Res.* **1998**, *37*, 1181.

(13) Bessel, S. Support effects in cobalt-based Fischer-Tropsch catalysts. *Appl. Catal., A* **1993**, *96*, 253.

(14) Bessell, S. ZSM-5 as a support for cobalt Fischer-Tropsch catalysts. *Stud. Surf. Sci. Catal.* **1994**, *81*, 461.

(15) Zhang, Z.; Sachtler, W. M. H.; Suib, S. L. Proximity requirement for Pd enhanced reducibility of Co^{2+} in NaY. *Catal. Lett.* **1989**, *2*, 395.

(16) Reuel, R. C.; Bartholomew, C. H. Effects of support and dispersion on the CO hydrogenation activity/selectivity properties of cobalt. *J. Catal.* **1984**, *85*, 78.

(17) Iglesia, E.; Soled, S. L.; Fiato, R. A. Fischer-Tropsch synthesis on cobalt and ruthenium. Metal dispersion and support effects on reaction rate and selectivity. *J. Catal.* **1992**, *137*, 212.

(18) Iglesia, E.; Reyes, S. C.; Madon, R. J.; Soled, S. L. *Advances in Catalysis and Related Subjects*; Academic Press: New York, 1993; Vol. 39, p 239.

(19) Anderson, R. B.; Hall, W. K.; Krieg, A.; Seligman, B. Studies of the Fischer-Tropsch synthesis. V. Activities and surface areas of reduced and carburized cobalt catalysts. *J. Am. Chem. Soc.* **1949**, *71*, 183.

(20) Diaz, U.; Fornes, V.; Corma, A. On the mechanism of zeolite growing: Crystallization by seeding with delayered zeolites. *Microporous Mesoporous Mater.* **2006**, *90*, 73.

(21) Corma, A.; Corell, C.; Pérez-Pariente, J. Synthesis and characterization of the MCM-22 zeolite. *Zeolites* **1995**, *15*, 2.

(22) Wang, C. B.; Lin, H. K.; Tang, C. W. Thermal characterization and microstructure change of cobalt oxides. *Catal. Lett.* **2004**, *94*, 69.

(23) Ishihara, T.; Horiuchi, N.; Eguchi, K.; Arai, H. Importance of surface hydrogen concentration in enhancing activity of Co-Ni alloy catalyst for Co hydrogenation. *J. Mol. Catal.* **1992**, *72*, 253.

(24) McDonald, M. A.; Storm, D. A.; Boudart, M. Hydrocarbon synthesis from Co-H_2 on supported iron: Effect of particle size and interstitials. *J. Catal.* **1986**, *102*, 386.

(25) Cullity, B. D. *Elements of X-ray Diffraction*; Addison-Wesley: London, 1978.

(26) Ernst, B.; Libs, S.; Chaumette, P.; Kiennemann, A. Preparation and characterization of Fischer-Tropsch active Co/SiO_2 catalysts. *Appl. Catal., A* **1999**, *186*, 145.

(27) Enache, D. I.; Rebours, B.; Roy-Auberger, M.; Revel, R. *In situ* XRD study of the influence of thermal treatment on the characteristics and the catalytic properties of cobalt-based Fischer-Tropsch catalysts. *J. Catal.* **2002**, *205*, 346.

(28) Arnoldy, P.; Moujlin, J. A. Temperature-programmed reduction of CoO/Al_2O_3 catalysts. *J. Catal.* **1985**, *93*, 38.

(29) Enache, D. I.; Roy-Auberger, M.; Revel, R. Differences in the characteristics and catalytic properties of cobalt-based Fischer-Tropsch catalysts supported on zirconia and alumina. *Appl. Catal., A* **2004**, *268*, 51.

(30) Khodakov, A. Y.; Griboval-Constant, A.; Bechara, R.; Zholobenko, V. L. Pore size effects in Fischer-Tropsch synthesis over cobalt-supported mesoporous silicas. *J. Catal.* **2002**, *206*, 230.

(31) Huang, Y. Y.; Anderson, J. R. On the reduction of supported iron catalysts studied by Mossbauer spectroscopy. *J. Catal.* **1975**, *40*, 143.

(32) Johnson, B. G.; Bartholomew, C. H.; Goodman, D. W. The role of surface structure and dispersion in CO hydrogenation on cobalt. *J. Catal.* **1991**, *128*, 231.

(33) Corma, A.; Orchilles, A. V. Formation of products responsible for motor and research octane of gasolines produced by cracking. The implication of framework Si/Al ratio and operation variables. *J. Catal.* **1989**, *115*, 551.

Received for review January 16, 2007
Revised manuscript received June 18, 2007
Accepted July 20, 2007

IE070099J